Discrete and Continuous Dynamical Systems - Series B

doi:10.3934/dcdsb.2022110

MODELLING *TRYPANOSOMA CRUZI*-*TRYPANOSOMA RANGELI* CO-INFECTION AND PATHOGENIC EFFECT ON CHAGAS DISEASE SPREAD

Xiaotian Wu

Colleges of Arts and Sciences, Shanghai Maritime University
Shanghai 201306, China

Daozhou Gao

Department of Mathematics, Shanghai Normal University
Shanghai 200234, China

Zilong Song

Department of Mathematics and Statistics, Utah State University
Logan, UT, 84322, United States

Jianhong Wu*

Department of Mathematics and Statistics, York University
Toronto, ON, M3J1P3, Canada

(Communicated by Dongmei Xiao)

Abstract. A mathematical model is developed to investigate the impact of *Trypanosoma cruzi* and *Trypanosoma rangeli* co-infection and *Trypanosoma rangeli*-induced pathogenicity of triatomine bugs on the spread of Chagas disease. Due to the presence of two parasites, basic reproduction numbers of one parasite in the absence of the other parasite ($\mathcal{R}_{10}$ and $\mathcal{R}_{20}$) and invasion reproduction numbers of one parasite invading the other parasite ($\mathcal{R}_{12}$ and $\mathcal{R}_{21}$) are derived to determine the dynamics of the co-infection system. With a simple case of two parasites' independent transmission, we have found that both parasites go extinct if both $\mathcal{R}_{i0} < 1\,(i = 1, 2)$, thus no Chagas disease spread. Nevertheless, the condition of $\mathcal{R}_{i0} > 1\,(i = 1, 2)$ is not sufficient to cause Chagas disease persistence, the invasion reproduction number of *Trypanosoma cruzi* invading *Trypanosoma rangeli* transmission $\mathcal{R}_{12}$ plays an important role. Specifically, Chagas disease could go extinct if $\mathcal{R}_{12} < 1$, and uniformly persistent if $\mathcal{R}_{12} > 1$. Moreover, due to pathogenicity, oscillation pattern of Chagas disease is observed, which is different from other mechanisms such as maturation delay, seasonality and regular spraying with insecticides for vector control. In conclusion, we have found that the presence of *Trypanosoma rangeli* infection leads to the risk reduction of Chagas disease infection. Our findings are beneficial to the prevention and control of Chagas disease.

2020 *Mathematics Subject Classification.* Primary: 92D25, 92D30; Secondary: 37N25.

Key words and phrases. Chagas disease, triatomine bugs, *Trypanosoma cruzi*, *Trypanosoma rangeli*, co-infection, pathogenic effect, oscillation pattern.

The work is supported by NSF of China (12071300), NSF of Shanghai (20ZR1440600), and NSERC of Canada and the Canada Research Chair program.

*Corresponding author: Jianhong Wu.

1. **Introduction.** Chagas disease is one of the most important zoonotic infections, caused by the infection with an etiological agent of *Trypanosoma cruzi (T. cruzi)* parasite. Humans and animals normally acquire the infection by contacting with faeces or urine of infected triatomine bugs during/after blood-sucking [9, 30, 37, 49]. Once the protozoan *T. cruzi* invades into the bloodstream, the infected individuals initially undergo an acute stage lasting one to two months, and around 5% infections may display clinical symptoms and infected patients can be treated by drugs such as benznidazole or nifurtimox [13, 30]. The majority of acute cases can progress into a chronic stage with a considerably variable duration from 10 to 30 years. During this stage, most patients never develop clinical symptoms, while a small portion may suffer from disease induced heart disease and associated complications [13, 30, 49].

In contrast, the impact of *Trypanosoma rangeli* (*T. rangeli*) on Chagas disease is secondary: *T. rangeli* shares with *T. cruzi* the large overlaps of geographical distribution, and the same mammalian hosts and triatomine species, particularly for example *Rhodnius prolixus* (*R. prolixus*) [39]. Despite being considered non-pathogenic to mammal hosts, *T. rangeli* is epidemiologically important for Chagas disease transmission since it may cause false-positive diagnosis of Chagas disease, and it is pathogenic to triatomine vectors, leading to the reduction of vector reproduction and survival [15, 19, 35]. This can alter the triatomine bugs population dynamics and subsequently alter the Chagas disease spreading process.

Due to the great epidemiological importance of *T. cruzi* and *T. rangeli*, and their co-infection is an important component for predicting and preventing Chagas disease transmission risk. Indeed, there are some biological evidences that prevalence of these two parasites co-infection at natural contiguous forests and domestic/peridomestic habitats is common for both vertebrate hosts and invertebrate traitomine bugs, particularly genus *Rhodnius* which are key vectors for propagating Chagas disease to humans [14, 17, 18, 20, 35, 48]. Moreover, biological studies of the effects of *T. cruzi* and *T. rangeli* co-infection on the fitness of triatomines *R. prolixus* and mammals are often reported [3, 4, 5, 6, 35]. Whereas, how to mathematically model this *T. cruzi* and *T. rangeli* co-infection and *T. rangeli*-induced pathogenicity of triatomine bugs and to evaluate their effects in the spread of Chagas disease have not been investigated to our best knowledge.

Significant progresses, involving *T. cruzi* transmission alone, have been made to model the dynamics and risk of Chagas disease transmission. These modeling studies have focused on: i). interaction between humans and triatomine vectors by taking into account different transmission routes and different stages of infection in human population [29, 46, 47]; ii). host community composition and host movement behaviors [1, 21, 23, 34, 44]; iii). the design and optimization of control intervention [7, 22, 26, 27, 28]. In a recent study, we investigated the dynamics of *T. rangeli* parasite relevant populations by considering the mutual interaction among *T. rangeli* parasites, competent and quasi-competent hosts, triatomine bugs, and co-feeding transmission [50]. That study observed the oscillatory behaviors of model solutions which is caused by the *T. rangeli*-induced infection for vector population, confirming the significance of *T. rangeli* parasites, contrary to the common belief that *T. rangeli* is of only secondary importance for Chagas disease transmission.

Based on our previous work, we aim to develop a mathematical model to describe the interplay among two parasites of *T. cruzi* and *T. rangeli*, vertebrate hosts which could be humans and wild/domestic animals, and genus *Rhodnius* traitomine bugs. We will determine the threshold conditions for the extinction and persistence of *T.*

cruzi parasite transmission, clarify the impact of co-infection on the risk of Chagas disease spread, and reveal certain unexpected phenomena such as fluctuation pattern. These, in turn, would have implications for vector control and prevention strategies of Chagas disease transmission.

The paper is organized as follows: a model of *T. cruzi* and *T. rangeli* co-infection and *T. rangeli*-induced pathogenic effects on triatomine bugs is formulated in Section 2. A basic result for the extinction of triatomine bug population is provided in Section 3. Some conditions for the extinction and persistence of Chagas disease are presented in Section 4. In Section 5, we present the main numerical results with an emphasis on the effect of co-infection and pathogenicity on Chagas disease spread. Finally, a discussion and conclusion will end our paper in Section 6.

2. Model formulation.

We propose a deterministic SI model describing the Chagas disease's host and vector interaction on the basis of *T. cruzi* and *T. rangeli* co-infection. Accordingly, both hosts and vectors are divided into susceptible and infected classes, while depending upon the states of parasite infection. Let $S_j(t)$, I_{j1}, $I_{j2}(t)$ and $I_{j3}(t)$ $(j = h, v)$ be the numbers of host and vector subpopulations who are susceptible, infected with *T. cruzi* parasites alone, *T. rangeli* parasites alone and both parasites at time t, respectively. In the following, indexes 0, 1, 2, 3 indicate the infection of no parasites, single *T. cruzi* parasites, single *T. rangeli* parasites, and both *T. cruzi* and *T. rangeli* parasites, respectively. .

2.1. Host population transmission dynamics.

Since animals infected with either parasite are non-pathogenic, and human mortality induced by Chagas protozoan *T. cruzi* is small, in this study we assume that the disease-induced death of host population is ignored which is the same as the work in [8]. We further assume that the simultaneous transmission of both *T. cruzi* and *T. rangeli* parasites is negligible in the sense that a susceptible host/vector who is bitten by a dually-infected vector/host can become infected with either *T. cruiz* or *T. rangeli* parasite. While, an individual who is already infected with one single type of parasites can become co-infected when it is bitten by its counterpart who infects with the other type of parasites. For simplicity, we assume that the total number of host population is constant as N_h, which is balanced by the constant recruitment rate Λ_h and the natural mortality rate μ_h.

Transmission of *T. rangeli* is entirely dependent on biting rates as the organism is transmitted via the salivary route. The transmission of *T. cruzi* to hosts does not really occur via biting but can be dependent on biting as transmission is stercorarial (via feces), where the vector bites the host, defecates and then infects the wound or mucous membranes. For simplicity, we assume transmission of both *T. cruzi* and *T. rangeli* depend on vectors' biting rate. Thus, to characterize the infection rate between hosts and vectors, let a be the total number of bites per triatomine bug per unit time, and $b^{hk}_{i\to j}\,(i, j = 0, 1, 2, 3; k = 1, 2)$ be the transmission probability of parasite-k per bite received by hosts, who are already infected with parasite-j received from triatomine bugs who are infected with parasite-i, hence the average transmission rate of parasite-k per host per vector is $\beta^{hk}_{i\to j} = (b^{hk}_{i\to j}a)/N_h$. Hence, the infection rate of susceptible hosts is given by

$$(\beta^{h1}_{1\to 0}I_{v1}(t) + \beta^{h1}_{3\to 0}I_{v3}(t))S_h(t) + (\beta^{h2}_{2\to 0}I_{v2}(t) + \beta^{h2}_{3\to 0}I_{v3}(t))S_h(t),$$

and the former term is the influx of host population infected with *T. cruzi* parasites alone and the latter for the host population infected with single *T. rangeli* parasites.

Meanwhile the host population with a single parasite infection can become co-infected when they encounter with the other parasite infected triatomine bugs or co-infected vectors. Specifically, single *T. cruzi* or *T. rangeli* infected host population become co-infected at rates

$$(\beta^{h2}_{2\to1}I_{v2}(t)+\beta^{h2}_{3\to1}I_{v3}(t))I_{h1}(t) \quad \text{and} \quad (\beta^{h1}_{1\to2}I_{v1}(t)+\beta^{h1}_{3\to2}I_{v3}(t))I_{h2}(t),$$

respectively. A schematic diagram of co-infection transmission in the host population is illustrated in Figure 1.

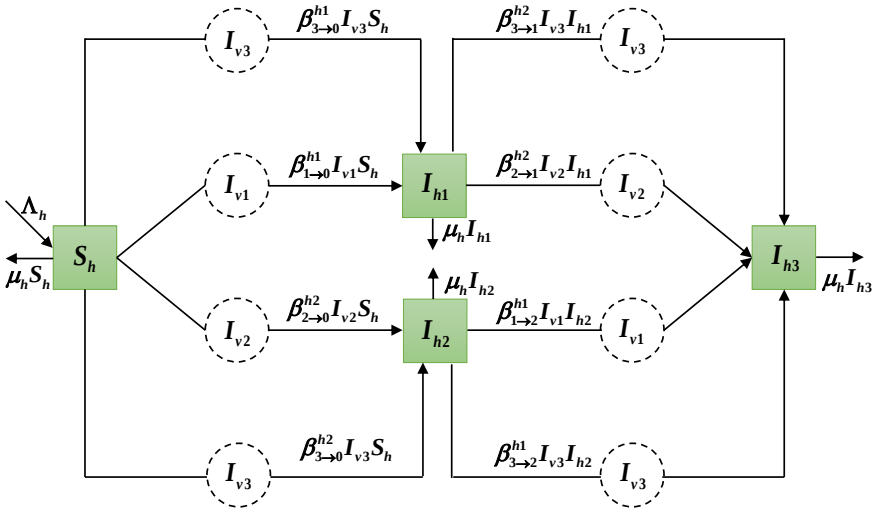

FIGURE 1. **(Color online) A schematic diagram of co-infection transmission in the host population.** Here S_h represents the subpopulation of susceptible hosts, and I_{hi}/I_{vi} $(i=1,2,3)$ represents the subpopulation of infected hosts/vectors with subscript i denoting the parasite infectious status, respectively. Subscript 0–no parasites; 1–single *T. cruzi* parasites; 2–single *T. rangeli* parasites; 3–both *T. cruzi* and *T. rangeli* parasites.

2.2. **Vector population transmission dynamics.** The transmission process of vector population is similar to that of host population. Let $b^{vk}_{i\to j}$ $(i,j=0,1,2,3;k=1,2)$ be transmission probability of parasite-k per contact, received by triatomine bugs who are infected with parasite-j sending from hosts who are infected with parasite-i, thus the average transmission rate of parasite-k per vector per host is $\beta^{vk}_{i\to j}=(b^{vk}_{i\to j}a)/N_h$. As the statement of host population co-infection transmission, we can similarly derive the infection rates of each triatomine bugs subpopulation. For example, the infection rate of susceptible vectors is

$$(\beta^{v1}_{1\to0}I_{h1}(t)+\beta^{v1}_{3\to0}I_{h3}(t))S_v(t)+(\beta^{v2}_{2\to0}I_{h2}(t)+\beta^{v2}_{3\to0}I_{h3}(t))S_v(t),$$

and others are similar.

As we mentioned in the introduction, *T. rangeli* is pathogenic to triatomine bugs which leads to the reduced fecundity and high mortality of the infected counterparts

[15, 34]. Accordingly, we denote by $\theta_i \in (0,1)$ the fecundity reduction and δ_{vi} $(i = 2,3)$ the corresponding *T. rangeli*-induced death rates of different triatomine bugs, respectively, which differ from their natural death rate μ_v. Following the Ricker-type function for the reproduction of triatomine vectors [38], the birth rate of susceptible bugs at time t is defined by:

$$b_v(t) = r\left(S_v(t) + I_{v1}(t) + \sum_{i=2}^{3}\theta_i I_{vi}(t)\right) e^{-\sigma\left(S_v(t)+\sum\limits_{i=1}^{3} I_{vi}(t)\right)}, \tag{1}$$

where r is the intrinsic birth rate of triatomine bug, and σ is density-dependent strength measuring the reproduction of bugs. This assumption reflects the ecological consideration that the reproduction is linear for the small size of triatomine population, decreases as a consequence of intraspecific competition, and then drops significantly at very large triatomine densities due to the limited resources. The schematic diagram of triatomine bug population transmission is illustrated in Figure 2.

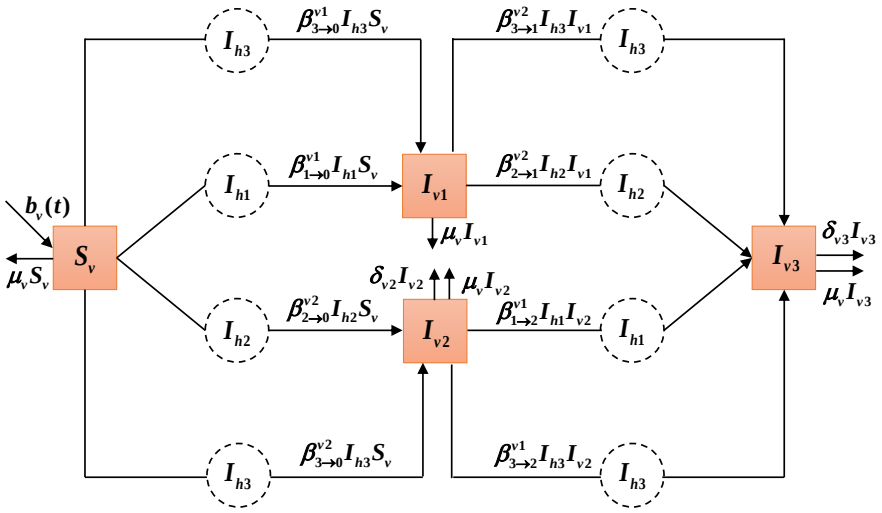

FIGURE 2. **(Color online) A schematic diagram of co-infection in the triatomine bug population.** Here S_v is the number of susceptible triatomine bugs and I_{vi}/I_{hi} $(i = 1,2,3)$ represents the number of infected triatomine bugs/hosts with subscript i denoting the infectious status with parasite-i, respectively. Subscript 0–no parasites; 1–single *T. cruzi* parasites; 2–single *T. rangeli* parasites; 3–both *T. cruzi* and *T. rangeli* parasites.

2.3. **Full system of host-vector interaction with two parasites co-infection.** According to the above statements and following the flowcharts of Fig. 1 and Fig. 2, the model describing the interaction among hosts, triatomine bugs and two types of parasites is given by the following system of ODEs:

$$
\begin{cases}
I'_{h1}(t) = \sum\limits_{i\in\{1,3\}} \beta^{h1}_{i\to 0} I_{vi}(t)\left(N_h - \sum\limits_{i\in\{1,2,3\}} I_{hi}(t)\right) \\
\qquad - \sum\limits_{i\in\{2,3\}} \beta^{h2}_{i\to 1} I_{vi}(t) I_{h1}(t) - \mu_h I_{h1}(t), \\
I'_{h2}(t) = \sum\limits_{i\in\{2,3\}} \beta^{h2}_{i\to 0} I_{vi}(t)\left(N_h - \sum\limits_{i\in\{1,2,3\}} I_{hi}(t)\right) \\
\qquad - \sum\limits_{i\in\{1,3\}} \beta^{h1}_{i\to 2} I_{vi}(t) I_{h2}(t) - \mu_h I_{h2}(t), \\
I'_{h3}(t) = \sum\limits_{i\in\{2,3\}} \beta^{h2}_{i\to 1} I_{vi}(t) I_{h1}(t) + \sum\limits_{i\in\{1,3\}} \beta^{h1}_{i\to 2} I_{vi}(t) I_{h2}(t) - \mu_h I_{h3}(t), \\
S'_v(t) = b_v(t) - \sum\limits_{i\in\{1,3\}} \beta^{v1}_{i\to 0} I_{hi}(t) S_v(t) - \sum\limits_{i\in\{2,3\}} \beta^{v2}_{i\to 0} I_{hi}(t) S_v(t) - \mu_v S_v(t), \\
I'_{v1}(t) = \sum\limits_{i\in\{1,3\}} \beta^{v1}_{i\to 0} I_{hi}(t) S_v(t) - \sum\limits_{i\in\{2,3\}} \beta^{v2}_{i\to 1} I_{hi}(t) I_{v1}(t) - \mu_v I_{v1}(t), \\
I'_{v2}(t) = \sum\limits_{i\in\{2,3\}} \beta^{v2}_{i\to 0} I_{hi}(t) S_v(t) - \sum\limits_{i\in\{1,3\}} \beta^{v1}_{i\to 2} I_{hi}(t) I_{v2}(t) - (\delta_{v2}+\mu_v) I_{v2}(t), \\
I'_{v3}(t) = \sum\limits_{i\in\{2,3\}} \beta^{v2}_{i\to 1} I_{hi}(t) I_{v1}(t) + \sum\limits_{i\in\{1,3\}} \beta^{v1}_{i\to 2} I_{hi}(t) I_{v2}(t) - (\delta_{v3}+\mu_v) I_{v3}(t),
\end{cases}
\tag{2}
$$

with $S_h(t) = N_h - I_{h1}(t) - I_{h2}(t) - I_{h3}(t)$, and $b_v(t)$ is the birth rate of triatomine bugs given in Eq. (1). All parameter values are assumed to be non-negative, and the corresponding biological explanations are detailed in Table 1.

Following Theorem 5.2.1 in [40] and similar idea for the boundedness in [50], we have drawn the following conclusion.

Proposition 1. *For any given non-negative initial value $x_0 \in \mathbb{R}^7_+$, model (2) has a unique solution which exists globally and is non-negative and bounded for all $t \geq 0$.*

3. **Extinction of triatomine bug population.** Vector-free equilibrium $E_v = (0,0,0,0,0,0,0)$ of system (2) always exists. Linearizing the system at E_v, we obtain the Jacobian matrix as

$$
J(E_v) = \begin{pmatrix}
-\mu_h & 0 & 0 & 0 & \beta^{h1}_{1\to 0} N_h & 0 & \beta^{h1}_{3\to 0} N_h \\
0 & -\mu_h & 0 & 0 & 0 & \beta^{h2}_{2\to 0} N_h & \beta^{h2}_{3\to 0} N_h \\
0 & 0 & -\mu_h & 0 & 0 & 0 & 0 \\
0 & 0 & 0 & r-\mu_v & r & r\theta_2 & r\theta_3 \\
0 & 0 & 0 & 0 & -\mu_v & 0 & 0 \\
0 & 0 & 0 & 0 & 0 & -(\delta_{v2}+\mu_v) & 0 \\
0 & 0 & 0 & 0 & 0 & 0 & -(\delta_{v3}+\mu_v)
\end{pmatrix}.
\tag{3}
$$

This implies that there is a positive eigenvalue if $r > \mu_v$ and all real eigenvalues are negative if $r < \mu_v$. Denote

$$
\mathcal{R}_v = r/\mu_v, \tag{4}
$$

which is a critical threshold characterizes the extinction and persistence of triatomine bug population.

Theorem 3.1. *For system (2) with any initial data $x_0 \in \mathbb{R}^7_+$, E_v is globally asymptotically stable if $\mathcal{R}_v < 1$ and unstable if $\mathcal{R}_v > 1$.*

Proof. It follows from the Jacobian matrix $J(E_v)$ that E_v is unstable if $\mathcal{R}_v > 1$ and locally asymptotically stable if $\mathcal{R}_v < 1$.

TABLE 1. **Parameter description and justification**

Parameter	Description	Range/Value	Source
N_h	total number of hosts	400	[29, 50]
a	number of bites per bug per unit time	$(0.2, 33)\, day^{-1}$	[36]
$b_{i\to j}^{hk}$	transmission probability of parasite-k per contact, from triatomine bugs who are infected with parasite-i to hosts who are already infected with parasite-j	[0.00271,0.06]	[29, 44]
$\beta_{i\to j}^{hk}$	transmission rate of parasite-k per host per vector, from triatomine bugs who are infected with parasite-i to hosts who are already infect with parasite-j	$(ab_{i\to j}^{hk})/N_h$	calculated
$b_{i\to j}^{vk}$	transmission probability of parasite-k per contact, from hosts who are infected with parasite-i to vectors who are already infected with parasite-j	[0.00026,0.49]	[1, 44]
$\beta_{i\to j}^{vk}$	transmission rate of parasite-k per host per vector, from hosts who are infected with parasite-i to vectors who are already infected with parasite-j	$(ab_{i\to j}^{vk})/N_h$	calculated
μ_h	host mortality rate	$[0.000038, 0.0025]\, day^{-1}$	[1, 44]
μ_v	vector mortality rate	$[0.0045, 0.0083]\, day^{-1}$	[1, 44]
r	the intrinsic birth rate of vectors	$[0.0274, 0.7714]\, day^{-1}$	[1, 29, 50]
σ	density-dependency strength measuring the reproduction of bugs	$[0, \infty)$	[50]
$\theta_i (i = 2, 3)$	*T. rangeli*-induced reproduction reduction of traitomine bugs who are infected with parasite-i	[0,1]	assumed
$\delta_{vi} (i = 2, 3)$	*T. rangeli*-induced mortality rate of traitomine bugs who are infected with parasite-i	$(0, 0.05]\, day^{-1}$	[2, 50]

Considering the total number of triatomine bug population by

$$N_v(t) = S_v(t) + I_{v1}(t) + I_{v2}(t) + I_{v3}(t),$$

we have

$$\begin{aligned} N_v'(t) &= r\left(S_v(t) + I_{v1}(t) + \sum_{i=2}^{3} \theta_i I_{vi}(t)\right) e^{-\sigma N_v(t)} - \sum_{i=2}^{3} \delta_{vi} I_{vi}(t) - \mu_v N_v(t) \\ &\le (re^{-\sigma N_v(t)} - \mu_v) N_v(t). \end{aligned}$$

In the case of $\mathcal{R}_v < 1$, we have

$$N_v'(t) \le (r - \mu_v) N_v(t),$$

yielding

$$\limsup_{t\to+\infty} N_v(t) \le \lim_{t\to+\infty} N_v(0) e^{\mu_v(\mathcal{R}_v - 1)t} = 0.$$

That is,

$$\lim_{t\to+\infty} N_v(t) = 0 \Leftrightarrow \lim_{t\to+\infty} S_v(t) = \lim_{t\to+\infty} I_{vi}(t) = 0,\ i = 1, 2, 3,$$

implying that each triatomine bug subpopulation exponentially decays to zero for any feasible initial condition in $\mathbb{R}^7_+$. Subsequently, the limiting system of each infected host subpopulation $I_{hi}\,(i = 1, 2, 3)$ satisfies

$$I'_{hi}(t) = -\mu_h I_{hi}(t) \Rightarrow \lim_{t\to\infty} I_{hi}(t) = \lim_{t\to\infty} I_{hi}(0)e^{-\mu_h t} = 0.$$

Accordingly, we obtain E_v is globally asymptotically stable if $\mathcal{R}_v < 1$. □

4. **Extinction and persistence of Chagas disease.** We are interested in the extinction and persistence of Chagas disease, hence $\mathcal{R}_v > 1$ is always assumed in the rest of the paper.

4.1. **Basic reproduction numbers and invasion reproduction numbers.** System (2) has a parasite-free equilibrium $E_0 = (0, 0, 0, N_v^*, 0, 0, 0)$, where $N_v^* = \frac{1}{\sigma}\ln\mathcal{R}_v$. Using the next generation matrix method in [10, 11, 45], we have

$$F = \begin{pmatrix} 0 & A \\ B & 0 \end{pmatrix} \quad \text{and} \quad V = \operatorname{diag}\left(\mu_h, \mu_h, \mu_h, \mu_v, \delta_{v2} + \mu_v, \delta_{v3} + \mu_v\right),$$

where

$$A = \begin{pmatrix} \beta^{h1}_{1\to0}N_h & 0 & \beta^{h2}_{3\to0}N_h \\ 0 & \beta^{h2}_{2\to0}N_h & \beta^{h2}_{3\to0}N_h \\ 0 & 0 & 0 \end{pmatrix}, \quad B = \begin{pmatrix} \beta^{v1}_{1\to0}N_v^* & 0 & \beta^{v1}_{3\to0}N_v^* \\ 0 & \beta^{v2}_{2\to0}N_v^* & \beta^{v2}_{3\to0}N_v^* \\ 0 & 0 & 0 \end{pmatrix}.$$

Hence, the threshold of model (2) is defined as the spectral radius of the next generation matrix FV^{-1}, which is

$$\mathcal{R}_0 = \rho(FV^{-1}) = \max\left\{\mathcal{R}_{10}, \mathcal{R}_{20}\right\},$$

where

$$\mathcal{R}_{10} = \sqrt{\frac{\beta^{h1}_{1\to0}N_h}{\mu_h}\frac{\beta^{v1}_{1\to0}N_v^*}{\mu_v}} \quad \text{and} \quad \mathcal{R}_{20} = \sqrt{\frac{\beta^{h2}_{2\to0}N_h}{\mu_h}\frac{\beta^{v2}_{2\to0}N_v^*}{\delta_{v2}+\mu_v}}.$$

Here $\mathcal{R}_{10}$ and $\mathcal{R}_{20}$ are the *T. cruzi* and *T. rangeli* basic reproduction numbers of system (2) in the absence of the other parasite infection, respectively.

It is worthwhile noting that, though a number of model parameters are involved in the co-infection model (2), $\mathcal{R}_0$ only depends on the dominant parameters which are used to determine the basic reproduction numbers of one parasite in the absence of the other parasite, respectively.

For system (2), it involves the interaction of two parasites, thus the ability of one parasite invading the other parasite transmission may play an important role to determine its dynamics [16, 33]. To do this, boundary equilibria of only one parasite presence must be analyzed and summarized below [50].

Proposition 2. *For system (2) and $\mathcal{R}_0 > 1$, we have:*

(i) if $\mathcal{R}_{10} > 1$, there is an equilibrium $E_1 = (I^*_{h1}, 0, 0, S^*_{v1}, I^*_{v1}, 0, 0)$ indicating T. cruzi parasite infection alone, where $I^*_{h1}, S^*_{v1}, I^*_{v1}$ can be explicitly determined by the system (2) in the absence of T. rangeli parasite.

(ii) if $\mathcal{R}_{20} > 1$, there is an equilibrium $E_2 = (0, I^*_{h2}, 0, S^*_{v2}, 0, I^*_{v2}, 0)$ indicating T. rangeli parasite infection alone, where I^*_{h2}, S^*_{v2} and I^*_{v2} are implicitly determined by the system (2) in the absence of T. cruzi parasite.

We assume that equilibrium E_2 exists, or equivalently $\mathcal{R}_{20} > 1$. Using the next generation matrix method [10, 11, 45], the vectors for the rate of the appearance of new infection by *T. cruzi* parasite and the rate of transition are found as:

$$\mathscr{F}(I_{h1}, I_{h3}, I_{v1}, I_{v3}) = \begin{pmatrix} (\beta^{h1}_{1\to 0} I_{v1} + \beta^{h1}_{3\to 0} I_{v3})(N_h - (I_{h1} + I^*_{h2} + I_{h3})) \\ \beta^{h1}_{1\to 2} I_{v1} I^*_{h2} + \beta^{h1}_{3\to 2} I_{v3} I^*_{h2} \\ \beta^{v1}_{1\to 0} I_{h1} S^*_{v2} + \beta^{v1}_{3\to 0} I_{h3} S^*_{v2} \\ \beta^{v1}_{1\to 2} I_{h1} I^*_{v2} + \beta^{v1}_{3\to 2} I_{h3} I^*_{v2} \end{pmatrix},$$

$$\mathscr{V}(I_{h1}, I_{h3}, I_{v1}, I_{v3}) = \begin{pmatrix} \beta^{h2}_{2\to 1} I^*_{v2} I_{h1} + \beta^{h2}_{3\to 1} I_{v3} I_{h1} + \mu_h I_{h1} \\ -\beta^{h2}_{2\to 1} I^*_{v2} I_{h1} - \beta^{h2}_{3\to 1} I_{v3} I_{h1} + \mu_h I_{h3} \\ \beta^{v2}_{2\to 1} I^*_{h2} I_{v1} + \beta^{v2}_{3\to 1} I_{h3} I_{v1} + \mu_v I_{v1} \\ -\beta^{v2}_{2\to 1} I^*_{h2} I_{v1} - \beta^{v2}_{3\to 1} I_{h3} I_{v1} + (\delta_{v3} + \mu_v) I_{v3} \end{pmatrix},$$

respectively.

The derivatives of $\mathscr{F}$ and $\mathscr{V}$ at $(I_{h1}, I_{h3}, I_{v1}, I_{v3}) = (0, 0, 0, 0)$ are thus

$$F_1 = D\mathscr{F}(0,0,0,0) = \begin{pmatrix} 0 & F_{12} \\ F_{21} & 0 \end{pmatrix} \quad \text{and} \quad V_1 = D\mathscr{V}(0,0,0,0) = \begin{pmatrix} V_{11} & 0 \\ 0 & V_{22} \end{pmatrix},$$

where

$$F_{12} = \begin{pmatrix} \beta^{h1}_{1\to 0}(N_h - I^*_{h2}) & \beta^{h1}_{3\to 0}(N_h - I^*_{h2}) \\ \beta^{h1}_{1\to 2} I^*_{h2} & \beta^{h1}_{3\to 2} I^*_{h2} \end{pmatrix}, \quad F_{21} = \begin{pmatrix} \beta^{v1}_{1\to 0} S^*_{v2} & \beta^{v1}_{3\to 0} S^*_{v2} \\ \beta^{v1}_{1\to 2} I^*_{v2} & \beta^{v1}_{3\to 2} I^*_{v2} \end{pmatrix},$$

and

$$V_{11} = \begin{pmatrix} \beta^{h2}_{2\to 1} I^*_{v2} + \mu_h & 0 \\ -\beta^{h2}_{2\to 1} I^*_{v2} & \mu_h \end{pmatrix}, \quad V_{22} = \begin{pmatrix} \beta^{v2}_{2\to 1} I^*_{h2} + \mu_v & 0 \\ -\beta^{v2}_{2\to 1} I^*_{h2} & \delta_{v3} + \mu_v \end{pmatrix}.$$

Subsequently, invasion reproduction number of Chagas disease intruding *T. rangeli* parasite transmission, denoted by $\mathcal{R}_{12}$, is given by the spectral radius of the non-negative matrix $F_1 V_1^{-1}$, i.e.,

$$\mathcal{R}_{12} = \rho(F_1 V_1^{-1}) = \sqrt{\frac{A_1 + \sqrt{A_1^2 - 4A_0}}{2}}, \tag{5}$$

where

$$\begin{aligned} A_1 =& \frac{N_h - I^*_{h2}}{(\delta_{v3} + \mu_v)(\beta^{v2}_{2\to 1} I^*_{h2} + \mu_v)} \left(\beta^{h1}_{1\to 0}(\delta_{v3} + \mu_v) + \beta^{h1}_{3\to 0}\beta^{v2}_{2\to 1} I^*_{h2}\right) \\ & \times \frac{S^*_{v2}}{\mu_h(\beta^{h2}_{2\to 1} I^*_{v2} + \mu_h)} \left(\beta^{v1}_{1\to 0}\mu_h + \beta^{v1}_{3\to 0}\beta^{h2}_{2\to 1} I^*_{v2}\right) \\ & + \frac{\beta^{h1}_{3\to 0}(N_h - I^*_{h2})}{\delta_{v3} + \mu_v} \frac{I^*_{v2}}{\mu_h(\beta^{h2}_{2\to 1} I^*_{v2} + \mu_h)} \left(\beta^{v1}_{1\to 2}\mu_h + \beta^{v1}_{3\to 2}\beta^{h2}_{2\to 1} I^*_{v2}\right) \\ & + \frac{I^*_{h2}}{(\delta_{v3} + \mu_v)(\beta^{v2}_{2\to 1} I^*_{h2} + \mu_v)} \frac{\beta^{v1}_{3\to 0} S^*_{v2}}{\mu_h} \left(\beta^{h1}_{1\to 2}(\delta_{v3} + \mu_v) + \beta^{h1}_{3\to 2}\beta^{v2}_{2\to 1} I^*_{h2}\right) \\ & + \frac{\beta^{h1}_{3\to 2} I^*_{h2}}{\delta_{v3} + \mu_v} \frac{\beta^{v1}_{3\to 2} I^*_{v2}}{\mu_h}, \end{aligned}$$

and

$$\begin{aligned} A_0 =& (\beta^{h1}_{1\to 0}\beta^{h1}_{3\to 2} - \beta^{h1}_{3\to 0}\beta^{h1}_{1\to 2})(\beta^{v1}_{1\to 0}\beta^{v1}_{3\to 2} - \beta^{v1}_{3\to 0}\beta^{v1}_{1\to 2}) \\ & \times \frac{I^*_{h2}(N_h - I^*_{h2})}{(\beta^{v2}_{2\to 1} I^*_{h2} + \mu_v)(\delta_{v3} + \mu_v)} \frac{I^*_{v2} S^*_{v2}}{\mu_h(\beta^{h2}_{2\to 1} I^*_{v2} + \mu_h)}. \end{aligned}$$

It is noted that $\mathcal{R}_{12}$ is essentially complicated, depending on all parameters of the co-infection model (2), which will be jointly used to determine the extinction and persistence of Chagas disease as shown below. The explicit formula of the invasion reproduction number of *T. rangeli* parasite $\mathcal{R}_{21}$ can be similarly derived by linearizing the system (2) at E_1, while we omit the details here.

4.2. **Theoretical results.** To have some rigorous mathematical results, we start with a simple case by assuming that transmission of each parasite is independent and pathogenic effect on triatomine bugs is equal since system (2) is very complicated, namely

$$\begin{aligned} &\beta_{i\to 0}^{m1}=\beta_{i\to 2}^{m1}=\beta_{m1},\ i=1,3, \quad \beta_{j\to 0}^{m2}=\beta_{j\to 1}^{m2}=\beta_{m2},\ j=2,3,\\ &\theta_2=\theta_3=\theta,\ \delta_{2v}=\delta_{3v}=\delta_v, \end{aligned} \tag{6}$$

where the symbol m is either h or v.

Firstly, it can be shown that

$$\Omega=\left\{(I_{h1},I_{h2},I_{h3},S_v,I_{v1},I_{v2},I_{v3})\in\mathbb{R}_+^7\,\middle|\,\sum_{i=1}^{3}I_{hi}\le N_h, S_v(t)+\sum_{i=1}^{3}I_{vi}\le N_v^*\right\}$$

is positively invariant with respect to system (2). Moreover, under the assumption (6), $\mathcal{R}_{10}$, $\mathcal{R}_{20}$ and $\mathcal{R}_{12}$ can be rewritten as

$$\mathcal{R}_{10}=\sqrt{\frac{\beta_{h1}N_h}{\mu_h}\frac{\beta_{v1}N_v^*}{\mu_v}},\quad \mathcal{R}_{20}=\sqrt{\frac{\beta_{h2}N_h}{\mu_h}\frac{\beta_{v2}N_v^*}{\delta_v+\mu_v}} \tag{7}$$

and

$$\mathcal{R}_{12}=\sqrt{\frac{\beta_{h1}N_h}{\delta_v+\mu_v}\frac{\beta_{v1}S_{v2}^*}{\mu_h}\frac{\delta_v+\mu_v+\beta_{v2}I_{h2}^*}{\beta_{v2}I_{h2}^*+\mu_v}+\frac{\beta_{h1}N_h}{\delta_v+\mu_v}\frac{\beta_{v1}I_{v2}^*}{\mu_h}}. \tag{8}$$

Remark 1. For system (2) under the assumption (6), we have $\mathcal{R}_{12}<\mathcal{R}_{10}$ and $\mathcal{R}_{20}=\mathcal{R}_{21}$.

Lemma 4.1. *For system (2) under the assumption (6), we have*

(i) If $\mathcal{R}_{10}<1$, then both $\lim_{t\to\infty}I_{hi}(t,x_0)=0$ and $\lim_{t\to\infty}I_{vi}(t,x_0)=0$ $(i=1,3)$ for $\forall x_0\in\Omega$.

(ii) If $\mathcal{R}_{20}<1$, then both $\lim_{t\to\infty}I_{hi}(t,x_0)=0$ and $\lim_{t\to\infty}I_{vi}(t)=0$ $(i=2,3)$ for $\forall x_0\in\Omega$.

Proof. The summations of I_{h1}' and I_{h3}', and of I_{v1}' and I_{v3}' of system (2) yield

$$\begin{cases} (I_{h1}+I_{h3})'(t)=\beta_{h1}(N_h-(I_{h1}+I_{h3}))(I_{v1}+I_{v3})-\mu_h(I_{h1}+I_{h3}),\\ (I_{v1}+I_{v3})'(t)=\beta_{v1}(S_v+I_{v2})(I_{h1}+I_{h3})-\delta_vI_{v3}-\mu_v(I_{v1}+I_{v3}). \end{cases}$$

Since Ω is positively invariant, the above system satisfies

$$\begin{cases} (I_{h1}+I_{h3})'(t)\le\beta_{h1}N_h(I_{v1}+I_{v3})-\mu_h(I_{h1}+I_{h3}),\\ (I_{v1}+I_{v3})'(t)\le\beta_{v1}N_v^*(I_{h1}+I_{h3})-\mu_v(I_{v1}+I_{v3}), \end{cases}$$

which is a linear system of differential inequalities with a coefficient matrix of

$$\begin{pmatrix} -\mu_h & \beta_{h1}N_h\\ \beta_{v1}N_v^* & -\mu_v \end{pmatrix}.$$

The trace of this matrix is strictly negative, and the determinant is

$$\mu_h\mu_v-\beta_{h1}N_h\beta_{v1}N_v^*=\mu_h\mu_v(1-\mathcal{R}_{10}^2)>0$$

because of $\mathcal{R}_{10} < 1$, which indicates that both eigenvalues of the matrix are negative. By the comparison principle [41], we have

$$\limsup_{t\to\infty} I_{hi}(t) = \limsup_{t\to\infty} I_{vi}(t) = 0, \quad i = 1, 3,$$

for any initial data in Ω.

Similarly, for the changes of $I_{hi}(t)$ $(i = 2, 3)$ and $I_{vi}(t)$ $(i = 2, 3)$, we have

$$\begin{cases} (I_{h2} + I_{h3})'(t) = \beta_{h2}(N_h - (I_{h2} + I_{h3}))(I_{v2} + I_{v3}) - \mu_h(I_{h2} + I_{h3}), \\ (I_{v2} + I_{v3})'(t) = \beta_{v2}(S_v + I_{v1})(I_{h2} + I_{h3}) - (\delta_v + \mu_v)(I_{v2} + I_{v3}), \end{cases}$$

which induces a linear system of differential inequalities

$$\begin{cases} (I_{h2} + I_{h3})' \le \beta_{h2} N_h (I_{v2} + I_{v3}) - \mu_h(I_{h2} + I_{h3}), \\ (I_{v2} + I_{v3})' \le \beta_{v2} N_v^* (I_{h2} + I_{h3}) - (\delta_v + \mu_v)(I_{v2} + I_{v3}), \end{cases} \tag{9}$$

by positive invariance of Ω. The matrix of (9) is

$$\begin{pmatrix} -\mu_h & \beta_{h2} N_h \\ \beta_{v2} N_v^* & -(\delta_v + \mu_v) \end{pmatrix},$$

its trace is strictly negative, and the determinant is

$$\mu_h(\delta_v + \mu_v) - \beta_{h2} N_h \beta_{v2} N_v^* = \mu_h(\delta_v + \mu_v)(1 - \mathcal{R}_{20}^2) > 0$$

due to $\mathcal{R}_{20} < 1$. This indicates that both eigenvalues of above matrix are negative. By the comparison principle [41], we have

$$\limsup_{t\to\infty} I_{hi}(t, x_0) = \limsup_{t\to\infty} I_{vi}(t, x_0) = 0, \quad i = 2, 3,$$

for any initial data $x_0 \in \Omega$. □

Following Lemma 4.1 and Theorems 4 and 6 in [50], we obtain the following results:

Theorem 4.2. *For system (2) under the assumption (6), we have*

(i) if $\mathcal{R}_0 = \max\{\mathcal{R}_{10}, \mathcal{R}_{20}\} < 1$, E_0 is globally asymptotically stable in Ω, i.e., Chagas disease goes extinct.

(ii) if $\mathcal{R}_{20} < 1 < \mathcal{R}_{10}$, E_1 is globally asymptotically stable in Ω, i.e., Chagas disease remains persistent.

(iii) if $\mathcal{R}_{10} < 1 < \mathcal{R}_{20}$, E_2 can be unstable in Ω, i.e., Chagas disease goes extinct, while T. rangeli parasite remains persistent.

Using Theorem 2 in [45], the following result is established.

Proposition 3. *When $\mathcal{R}_{20} = \mathcal{R}_{21} > 1$ and $\mathcal{R}_{10} > 1 > \mathcal{R}_{12}$, E_2 is locally asymptotically stable, i.e., Chagas disease cannot invade the T. rangeli parasite transmission.*

Following Theorem 4.6 by Thieme [43] and Theorem 2.4 by Zhao [51], we now establish the condition for coexistence equilibrium and uniform persistence of two parasites.

Theorem 4.3. *When $\mathcal{R}_{20} = \mathcal{R}_{21} > 1$ and $\mathcal{R}_{10} > \mathcal{R}_{12} > 1$, system (2) under assumption (6) admits at least one coexistence equilibrium $E^* = (\hat{I}_{h1}^*, \hat{I}_{h2}^*, \hat{I}_{h3}^*, \hat{S}_v^*, \hat{I}_{v1}^*, \hat{I}_{v2}^*, \hat{I}_{v3}^*)$ and both parasites are uniformly persistent, i.e., there is a constant $\kappa > 0$ such that each solution $\Phi_t(x_0) = (I_{h1}(t), I_{h2}(t), I_{h3}(t), S_v(t), I_{v1}(t), I_{v2}(t), I_{v3}(t))$ starting with an initial data $x_0 = (I_{h1}(0), I_{h2}(0), I_{h3}(0), S_v(0), I_{v1}(0), I_{v2}(0), I_{v3}(0)) \in \Omega_0$ satisfies*

$$\liminf_{t\to\infty} I_{hi}(t) > \kappa \quad \text{and} \quad \liminf_{t\to\infty} I_{vi}(t) > \kappa, \ i = 1, 2, 3,$$

where

$$\Omega_0 = \{x \in \Omega : \textit{at least one of } I_{m1}I_{n2} > 0 \textit{ for } m,n \in \{h,v\} \quad \textit{or } (I_{h3}, I_{v3}) \neq (0,0)\}$$

showing the simultaneous presence of two parasites.

Proof. For each $x = (I_{h1}, I_{h2}, I_{h3}, S_v, I_{v1}, I_{v2}, I_{v3}) \in \Omega$ of system (2), denote

$$\Omega_0 = \{x \in \Omega : \text{at least one of } I_{m1}I_{n2} > 0 \text{ for } m,n \in \{h,v\} \quad \text{or } (I_{h3}, I_{v3}) \neq (0,0)\}$$

and

$$\begin{aligned}\partial\Omega_0 = \Omega\backslash\Omega_0 = \{&x \in \Omega : (I_{h1}, I_{v1}) = (0,0) \text{ or } (I_{h2}, I_{v2}) = (0,0),\\ &\text{and } (I_{h3}, I_{v3}) = (0,0)\},\end{aligned}$$

such that $\Omega_0 \cap \partial\Omega_0 = \emptyset$.

It is sufficient to show that system (2) under assumption (6) is uniformly persistent with respect to $(\Omega_0, \partial\Omega_0)$. It is clear that Ω and Ω_0 are positively invariant and system (2) is point dissipative.

Let $M_\partial = \{x_0 \in \partial\Omega_0 : \Phi_t(x_0) \in \partial\Omega_0 \text{ for } t \geq 0\}$. Therefore, $M_\partial = \partial\Omega_0$. The boundary equilibria E_0, E_1, E_2 are in M_∂. Let $W^s(E_i)$ be the stable manifold of E_i for $i = 0,1,2$. We will show that $W^s(E_i) \cap \Omega_0 = \emptyset$ whenever $\mathcal{R}_{10} > \mathcal{R}_{12} > 1$ and $\mathcal{R}_{20} > 1$.

Define

$$\mathcal{R}_{10}^{\varepsilon} = \sqrt{\frac{\beta_{h1}(N_h - 3\varepsilon)}{2\beta_{h1}\varepsilon + \mu_h}\frac{\beta_{v1}(N_v^* - \varepsilon)}{2\beta_{v2}\varepsilon + \mu_v}}.$$

It follows from $\mathcal{R}_{10} > 1$ that there is an $\varepsilon_0 > 0$ such that $\mathcal{R}_{10}^{\varepsilon} > 1$ for $\varepsilon \in [0, \varepsilon_0]$. Let η_0 small enough such that

$$S_v(0) > N_v^* - \varepsilon_0 \text{ for } \|x_0 - E_0\| \leq \eta_0.$$

We claim that $\limsup_{t\to\infty} \|\Phi_t(x_0) - E_0\| > \eta_0$ for $x_0 \in \Omega_0$, where $\|\cdot\|$ is the Euclidean norm. Supposing not, then by translation, we have $\|\Phi_t(x_0) - E_0\| \leq \eta_0$ for all $t \geq 0$ and hence

$$\begin{aligned}I'_{h1}(t) &= \beta_{h1}(I_{v1} + I_{v3})(N_h - (I_{h1} + I_{h2} + I_{h3})) - \big[\beta_{h2}(I_{v2} + I_{v3}) + \mu_h\big]I_{h1}\\ &\geq \beta_{h1}I_{v1}(N_h - (I_{h1} + I_{h2} + I_{h3})) - \big[\beta_{h2}(I_{v2} + I_{v3}) + \mu_h\big]I_{h1}(t)\\ &\geq \beta_{h1}(N_h - 3\varepsilon_0)I_{v1} - (2\beta_{h2}\varepsilon_0 + \mu_h)I_{h1}, \qquad (10)\end{aligned}$$

and

$$\begin{aligned}I'_{v1}(t) &= \beta_{v1}(I_{h1} + I_{h3})S_v - \big[\beta_{v2}(I_{h2} + I_{h3}) + \mu_v\big]I_{v1}\\ &\geq \beta_{v1}I_{h1}S_v - \big[\beta_{v2}(I_{h2} + I_{h3}) + \mu_v\big]I_{v1}\\ &\geq \beta_{v1}(N_v^* - \varepsilon_0)I_{h1} - (2\beta_{h2}\varepsilon_0 + \mu_v)I_{v1}. \qquad (11)\end{aligned}$$

Combining (10) and (11) yields a planar homogeneous linear system of differential inequalities with a matrix of

$$J_0 = \begin{pmatrix} -(2\beta_{h2}\varepsilon_0 + \mu_h) & \beta_{h1}(N_h - 3\varepsilon_0) \\ \beta_{v1}(N_v^* - \varepsilon_0) & -(2\beta_{h2}\varepsilon_0 + \mu_v)\end{pmatrix}.$$

Its determinant is

$$\begin{aligned}\det(J_0) =&(2\beta_{h2}\varepsilon_0 + \mu_h)(2\beta_{h2}\varepsilon_0 + \mu_v)\left(1 - \frac{\beta_{h1}(N_h - 3\varepsilon_0)\beta_{v1}(N_v^* - \varepsilon_0)}{(2\beta_{h2}\varepsilon_0 + \mu_h)(2\beta_{h2}\varepsilon_0 + \mu_v)}\right)\\ =&(2\beta_{h2}\varepsilon_0 + \mu_h)(2\beta_{h2}\varepsilon_0 + \mu_v)(1 - (\mathcal{R}_{10}^{\varepsilon_0})^2) < 0\end{aligned}$$

because of $\mathcal{R}_{10}^{\varepsilon_0} > 1$. Hence, J_0 has a positive eigenvalue. By a comparison theorem [41], we have $I_{h1}(t)$ and $I_{v1}(t) \to \infty$ as $t \to \infty$, which yields a contradiction to the boundedness of system (2).

To show $W^s(E_1) \cap \Omega_0 = \emptyset$. Similarly, define

$$\mathcal{R}_{20}^{\varepsilon} = \sqrt{\frac{\beta_{h2}(N_h - 2\varepsilon)}{\mu_h} \frac{\beta_{v2}(N_v^* - 2\varepsilon)}{\delta_v + \mu_v}}.$$

It follows from $\mathcal{R}_{20} > 1$ that there is an $\varepsilon_1 > 0$ such that $\mathcal{R}_{20}^{\varepsilon} > 1$ for $\varepsilon \in [0, \varepsilon_1]$. Let η_1 small enough such that

$$S_{v1}^*+\varepsilon_1 > S_v(0) > S_{v1}^*-\varepsilon_1,\ I_{h1}^*+\varepsilon_1 > I_{h1}(0) > I_{h1}^*-\varepsilon_1,\ I_{v1}^*+\varepsilon_1 > I_{v1}(0) > I_{v1}^*-\varepsilon_1$$

for $\|x_0 - E_1\| \le \eta_1$.

We claim that $\limsup_{t\to\infty} \|\Phi_t(x_0) - E_1\| > \eta_1$ for $x_0 \in \Omega_0$. Supposing not, then by translation, we have $\|\Phi_t(x_0) - E_1\| \le \eta_1$ for all $t \ge 0$ and hence

$$\begin{aligned}(I_{h2} + I_{h3})'(t) &= \beta_{h2}(I_{v2} + I_{v3})(N_h - (I_{h2} + I_{h3})) - \mu_h(I_{h2} + I_{h3}) \\ &\ge \beta_{h2}(N_h - 2\varepsilon_1)(I_{v2} + I_{v3}) - \mu_h(I_{h2} + I_{h3}).\end{aligned} \tag{12}$$

Since $S_{v1}^* + I_{v1}^* = N_v^*$, we have

$$\begin{aligned}(I_{v2} + I_{v3})'(t) &= \beta_{v2}(I_{h2} + I_{h3})(S_v + I_{v1}) - (\delta_v + \mu_v)(I_{v2} + I_{v3}) \\ &\ge \beta_{v2}(N_v^* - 2\varepsilon_1)(I_{h2} + I_{h3}) - (\delta_v + \mu_v)(I_{v2} + I_{v3}).\end{aligned} \tag{13}$$

Combining (12) and (13) yields a planar homogeneous linear system of differential inequalities with a matrix of

$$J_1 = \begin{pmatrix} -\mu_h & \beta_{h2}(N_h - 2\varepsilon_1) \\ \beta_{v2}(N_v^* - 2\varepsilon_1) & -(\delta_v + \mu_v) \end{pmatrix}.$$

The trace of J_1 is negative, and the determinant is

$$\begin{aligned}\det(J_1) &= \mu_h(\delta_v + \mu_v)\left(1 - \frac{\beta_{h2}(N_h - 2\varepsilon_1)\beta_{v2}(N_v^* - 2\varepsilon_1)}{\mu_h(\delta_v + \mu_v)}\right) \\ &= \mu_h(\delta_v + \mu_v)\left(1 - (\mathcal{R}_{20}^{\varepsilon_1})^2\right) < 0\end{aligned}$$

because of $\mathcal{R}_{20}^{\varepsilon_1} > 1$. Hence, J_1 has a positive eigenvalue. By a comparison theorem [41], we have $(I_{h2} + I_{h3})(t)$, $(I_{v2} + I_{v3})(t) \to \infty$ as $t \to \infty$, a contradiction.

To show $W^s(E_2) \cap \Omega_0 = \emptyset$. Define

$$J_\varepsilon = F_1 - V_1 - \varepsilon\Delta \quad \text{and} \quad \Delta = \begin{pmatrix} -2\beta_{h2} & 0 & 3\beta_{h1} & 3\beta_{h1} \\ -2\beta_{h2} & 0 & \beta_{h1} & \beta_{h1} \\ \beta_{v1} & \beta_{v1} & -2\beta_{v2} & 0 \\ \beta_{v1} & \beta_{v1} & -2\beta_{v2} & 0 \end{pmatrix}.$$

Since $s(F_1 - V_1) > 0$ if and only if $\mathcal{R}_{12} > 1$, there is an $\varepsilon_2 > 0$ such that $s(J_\varepsilon) > 0$ for $\varepsilon \in [0, \varepsilon_2]$. We choose $x_0 \in \Omega_0$ and η_2 small enough such that

$$S_{v2}^*+\varepsilon_2 > S_v(0) > S_{v2}^*-\varepsilon_2,\ I_{h2}^*+\varepsilon_2 > I_{h2}(0) > I_{h2}^*-\varepsilon_2,\ I_{v2}^*+\varepsilon_2 > I_{v2}(0) > I_{v2}^*-\varepsilon_2$$

for $\|x_0 - E_2\| \le \eta_2$.

We then claim that $\limsup_{t\to\infty} \|\Phi_t(x_0) - E_2\| > \eta_2$ for the $x_0 \in \Omega_0$. Suppose not, then by translation, we have $\|\Phi_t(x_0) - E_2\| \le \eta_2$ for all $t \ge 0$ and hence

$$\begin{aligned}I'_{h1}(t) &\ge \beta_{h1}(N_h - I_{h2}^* - 3\varepsilon_2)(I_{v1}(t) + I_{v3}(t)) - \beta_{h2}(I_{v2}^* + 2\varepsilon_2 + \mu_h)I_{h1}(t), \\ I'_{h3}(t) &\ge \beta_{h1}(I_{h2}^* - \varepsilon_2)(I_{v1}(t) + I_{v3}(t)) + \beta_{h2}(I_{v2}^* - 2\varepsilon_2)I_{h1}(t) - \mu_h I_{h3}(t),\end{aligned}$$

$$I'_{v1}(t) \geq \beta_{v1}(S^*_{v2} - \varepsilon_2)(I_{h1}(t) + I_{h3}(t)) - \beta_{v2}(I^*_{h2} + 2\varepsilon_2 + \mu_v)I_{v1}(t),$$
$$I'_{v3}(t) \geq \beta_{v1}(I^*_{v2} - \varepsilon_2)(I_{h1}(t) + I_{h3}(t)) + \beta_{v2}(I^*_{h2} - 2\varepsilon_2)I_{v1}(t) - (\delta_v + \mu_v)I_{v3}(t).$$

Notice that J_ε has a positive eigenvalue $s(J_\varepsilon)$ associated to a positive eigenvector. It follows from a comparison theorem that $I_{h1}(t)$, $I_{h3}(t)$, $I_{v1}(t)$, and $I_{v3}(t) \to \infty$ as $t \to \infty$, a contradiction. Accordingly, system (2) under assumption (6) is uniformly weak persistent with respect to $(\Omega_0, \partial\Omega_0)$.

Since $W^s(E_0) = \{E_0\}$, $W^s(E_1) = \{E_1\}$, $W^s(E_2) = \{E_2\}$, and $M_\partial = W^s(E_0) \cup W^s(E_1) \cup W^s(E_2)$, $\{E_0\}$, $\{E_1\}$ and $\{E_2\}$ are isolated invariant sets and acyclic in M_∂. By Theorem 4.6 in Thieme [43], system (2) under assumption (6) is uniformly persistent with respect to $(\Omega_0, \partial\Omega_0)$. Moreover, by Theorem 2.4 in Zhao [51], system (2) under assumption (6) has an equilibrium $E^* = (\hat{I}^*_{h1}, \hat{I}^*_{h2}, \hat{I}^*_{h3}, \hat{S}^*_v, \hat{I}^*_{v1}, \hat{I}^*_{v2}, \hat{I}^*_{v3}) \in \Omega_0$ and it is easy to check that E^* is a positive equilibrium of system (2) under assumption (6). □

5. Simulation results.

In this section, we numerically present the results of *T. cruzi* and *T. rangeli* co-infection and pathogenic effect on Chagas disease spread. The model parameter values chosen for simulations are stemmed from Table 1 and under the assumption (6).

5.1. Impact of transmission rates on basic/invasive reproduction numbers.

As shown in Section 4, the basic/invasive reproduction numbers $\mathcal{R}_{i0}$ $(i = 1, 2)$ and $\mathcal{R}_{12}$ jointly determine the dynamics of the co-infection Chagas disease model (2). Now we consider how transmission rates between hosts and vectors alter the variation of $\mathcal{R}_{10}$, $\mathcal{R}_{20}$ and $\mathcal{R}_{12}$. Since the transmission rates between hosts and vectors are proportional to the biting rate a which has a wide range [36], we hence take the parameter a as an illustration. Figure 3 presents the impact of biting rate a on the basic/invasive reproduction numbers $\mathcal{R}_{10}$, $\mathcal{R}_{20}$ and $\mathcal{R}_{12}$. It is observed in Fig. 3 that, as the biting rate a increases, both $\mathcal{R}_{10}$ and $\mathcal{R}_{20}$ increase, while $\mathcal{R}_{12}$ increases initially, reaches the maximum value and then finally decreases below unity. This implies that large contact between hosts and vectors can give rise to the increase of both $\mathcal{R}_{10}$ and $\mathcal{R}_{20}$, while inadvertently leads to the decrease of the invasive reproduction number $\mathcal{R}_{12}$, even below unity.

5.2. Eradication of Chagas disease.

Figure 4 presents the comparison of Chagas disease spread with and without *T. rangeli*-involved co-infection. Fig. 4(a) and Fig. 4(b) display that, if *T. rangeli* parasites are absent, both population sizes of *T. cruzi*-infected hosts and triatomine bugs converge to positive, where $\mathcal{R}_{10} = 1.1060 > 1$, indicating the persistence of Chagas disease. However, if *T. rangeli* parasites are taken into account, Fig. 4(c) and Fig. 4(d) show that *T. cruzi*-infected population sizes eventually go extinct, where $\mathcal{R}_{10}$ is the same as 1.1060, $\mathcal{R}_{20} = 2.0163 > 1$ and $\mathcal{R}_{12} = 0.9364 < 1$. This reveals that *T. cruzi*-*T. rangeli* co-infection can lead to the eradication of Chagas disease.

This finding provides a theoretically plausible control strategy for Chagas disease elimination as long as $\mathcal{R}_{20} > 1$ and $\mathcal{R}_{10} > 1 > \mathcal{R}_{12}$ are satisfied. Moreover, by their explicit formulae given in Eqs. (7), $\mathcal{R}_{10}$ is independent of θ and δ_v, $\mathcal{R}_{20}$ is decreasing with respect to δ_v while irrelevant to θ, whereas $\mathcal{R}_{12}$ is closely related to these two parameters. Consequently, if there are certain values of θ and δ_v such that $\mathcal{R}_{20} > 1$ and $\mathcal{R}_{12} < 1 < \mathcal{R}_{10}$, one can eliminate *T. cruzi* parasites, confirming pathogenic effect plays an important role for the control and prevention of Chagas disease.

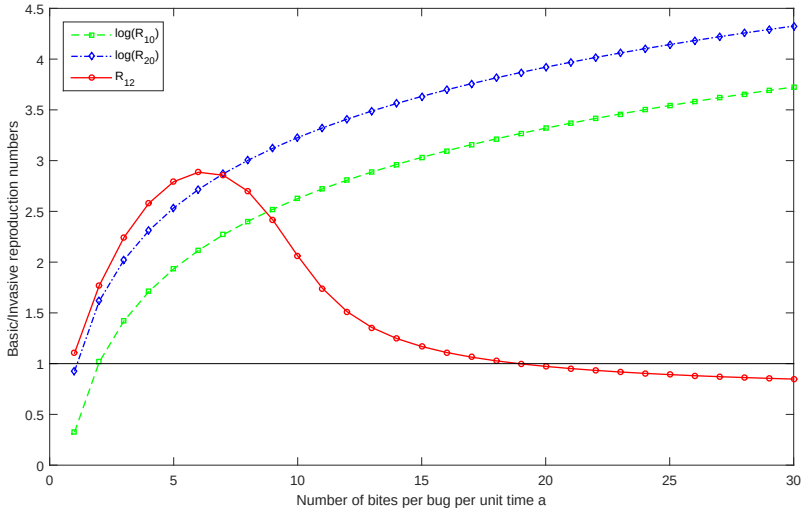

FIGURE 3. **(Color online) Impact of biting rate per bug per unit time on basic/invasive reproduction numbers.** Here, $a \in [1, 30]$, $N_h = 400$, $b^{h1}_{1\to 0} = 0.003$, $b^{h2}_{2\to 0} = 0.0027$, $b^{v1}_{1\to 0} = 0.00032$, $b^{v2}_{2\to 0} = 0.0026$, $\mu_h = 0.0005$, $\mu_v = 0.005$, $r = 0.03$, $\sigma = 0.0009$, $\theta = 0.01$, $\delta_v = 0.006$ are used.

5.3. **Reduction of Chagas disease risk.** We now proceed with the analysis of Chagas disease risk if *T. cruzi*-infected populations are established, by examining the case of $\mathcal{R}_{20} > 1$, $\mathcal{R}_{10} > 1$, and additional $\mathcal{R}_{12} > 1$. In this case, both *T. cruzi* and *T. rangeli* parasites are uniformly persistent, while the dynamical behavior of this co-existence equilibrium is uncertain. In fact, it can be unstable. We firstly test the stability of the equilibrium to examine the risk of Chagas disease spread. With the feasible values in Table 1 and three different initial data $x_1 = (10, 50, 50, 100, 10, 100, 10)$, $x_2 = (150, 100, 10, 100, 100, 100, 100)$ and $x_3 = (50, 10, 0, 200, 10, 200, 0)$ from the positively invariant set Ω, it is observed that all solutions stabilize at the same level (figure not shown). With this stable state, the basic reproduction numbers of *T. cruzi* and *T. rangeli* and the invasion reproduction number of *T. cruzi* are calculated as $\mathcal{R}_{10} = 8.3003 > 1$, $\mathcal{R}_{20} = 5.1230 > 1$, and $\mathcal{R}_{12} = 1.5174 > 1$, respectively.

Figure 5 shows the risk of Chagas disease in the presence and/or absence of *T. rangeli*-involved co-infection. It is noticed that the sizes of *T. cruzi*-infected host and triatomine bug populations in the case of co-infection are largely reduced as shown in Fig. 5(a,c), where red solid lines are below the corresponding blue dashed ones. Moreover, the population sizes of susceptible triatomine bugs are largely reduced as well due to the presence of *T. rangeli*-involved co-infection (see Fig. 5(b)). These phenomena indicate that involvement of *T. rangeli* parasite infection leads to the reduction of Chagas disease risk, further confirming that pathogenic effect on triatomine bugs plays a key role.

5.4. **Oscillation occurrence of Chagas disease.** Figure 6 exhibits the sustained oscillation pattern of *T. cruzi*-infected total host population when $\mathcal{R}_{10} > 1$, $\mathcal{R}_{20} > 1$ and $\mathcal{R}_{12} > 1$. Fig. 6(a) shows the influence of reproduction reduction θ on the

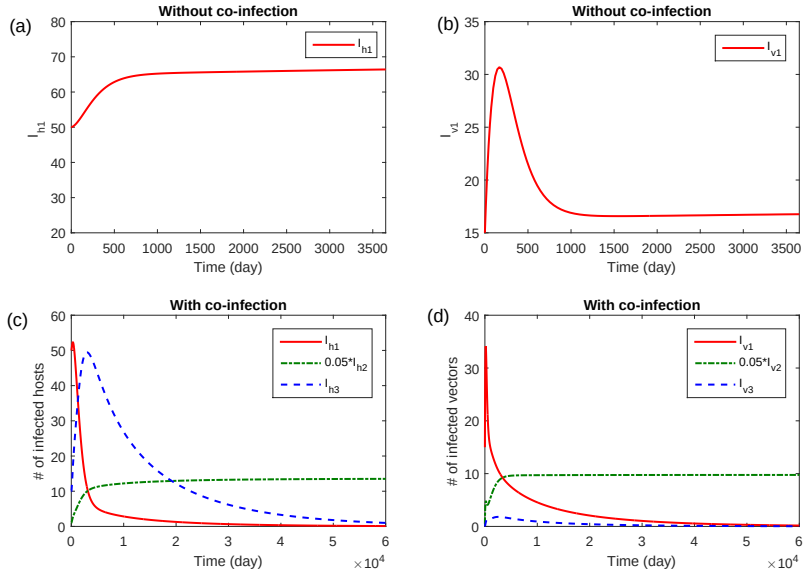

FIGURE 4. **(Color online) Impact of *T. rangeli* presence on the spread of Chagas disease if $\mathcal{R}_{20} > 1$ and $\mathcal{R}_{10} > 1 > \mathcal{R}_{12}$ are satisfied.** (a) and (b) are simulated from the model of *T. cruzi*-infection alone, and (c) and (d) are simulated from the co-infection model (2). Here, $a = 0.8$, $N_h = 400$, $b^{h1}_{1\to 0} = 0.003$, $b^{h2}_{2\to 0} = 0.0027$, $b^{v1}_{1\to 0} = 0.00032$, $b^{v2}_{2\to 0} = 0.0026$, $\mu_h = 0.0005$, $\mu_v = 0.005$, $r = 0.03$, $\sigma = 0.0009$, $\theta = 0.01$, $\delta_v = 0.006$ are used for the simulations.

solution of *T. cruzi*-infected host population. It is observed that stronger pathogenic effect of reproduction reduction (namely, smaller θ value) leads to larger oscillation period and amplitude of Chagas disease. Fig. 6(b) shows the influence of *T. rangeli*-induced death rate of triatomine bugs δ_v on the behavior of *T. cruzi*-infected host population. It is also noticed that as pathogenic effect of *T. rangeli*-induced death rate becomes stronger (namely, larger δ_v), the oscillation period and amplitude become larger. While, if we enlarge the life span of host population (namely, smaller μ_h), we observe that the oscillation period and amplitude become larger (Fig. 6(c)). We have to mention that, if triatomine bugs has no *T. rangeli*-induced pathogenic effect (i.e., $\theta = 1$ and $\delta_v = 0$), no damped oscillation is observed (figure not shown here), confirming pathogenic effect plays a critical role for the occurrence of Chagas disease oscillation pattern.

Despite the oscillation pattern is numerically explored in Fig. 6, it is hard to analytically identify the threshold condition. In order to have an intuitive view for the disappearance or occurrence of sustained oscillation, we perform some simulations to numerically identify the bifurcation diagram which is shown in Figure 7. It is noticed that small θ results in the appearance of oscillation since the minimum and maximum values of *T. cruzi*-infected host population at steady state are unequal, moreover smaller θ leads to larger oscillation (Figure 7(a)). Phenomenon of Fig. 7(b) is unexpected, in which it shows that both small and large values

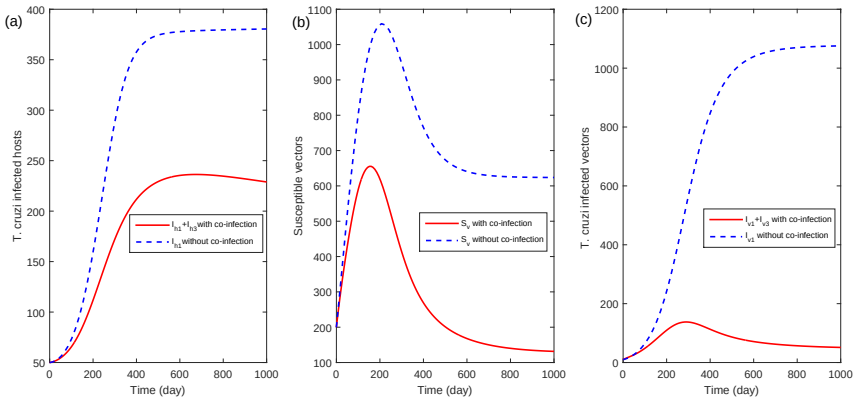

FIGURE 5. **(Color online) Impact of *T. cruzi* and *T. rangeli* co-infection on the risk of Chagas disease if $\mathcal{R}_{20} > 1$ and $\mathcal{R}_{10} > \mathcal{R}_{12} > 1$ are satisfied.** (a) Solutions of *T. cruzi*-infected hosts with/without co-infection; (b) solutions of susceptible vectors with/without co-infection; (c) solutions of *T. cruzi*-infected vectors with/without co-infection. Model parameters are $a = 0.3$, $N_h = 400$, $b^{h1}_{1\to 0} = 0.03$, $b^{v1}_{1\to 0} = 0.03$, $b^{h2}_{2\to 0} = 0.012$, $b^{v2}_{2\to 0} = 0.2$, $\mu_h = 0.001$, $\mu_v = 0.005$, $r = 0.0274$, $\sigma = 0.001$, $\theta = 0.9$, $\delta_v = 0.03$. Particularly, $b^{h2}_{2\to 0} = b^{v2}_{2\to 0} = \delta_v = 0$ and $\theta = 1$ in the case of no *T. rangeli* co-infection.

of *T. rangeli*-induced death rate can lead to the disappearance of Chagas disease oscillation.

6. **Discussion.** Motivated by two epidemiological important parasites of Chagas disease, we have developed a novel mathematical model to study their potential impact to Chagas disease spread. These two parasites, *T. cruzi* and *T. rangeli*, have a capacity to co-infect their vertebrate mammals and invertebrate triatomine bugs, while their corresponding pathological diagnosis is different, which attracts our attention. In contrast to *T. cruzi*, *T. rangeli* is non-pathogenic to human beings, while it influences the bugs' fitness giving rise to a significant reduction of reproduction and *T. rangeli*-induced death rate, thus alter the dynamics of triatomine bugs population [35]. In the present study, our aim is to focus on the biological implication of two parasites coinfection and pathogenic effect on Chagas disease spread.

For the high dimensional system, we have derived certain explicit formulae of critical thresholds: basic reproduction numbers of triatomine bug population $\mathcal{R}_v$ and of parasite population $\mathcal{R}_0$, and invasion reproduction numbers $\mathcal{R}_{12}$ and $\mathcal{R}_{21}$. These thresholds jointly determine the dynamics of the Chagas disease transmission model, thus for the implication of Chagas disease risk reduction. We have found that, if $\mathcal{R}_v < 1$, triatomine bugs population goes to extinction which is simple (see Theorem 3.1), implying no risk of Chagas disease. Due to the involvement of a number of model parameters, the dynamics of the developed model (2) is very complex, we thus have limited to a simple case in the current study that assuming the transmission of each parasite is independent. With this assumption (6), it is interesting to notice that, if $\mathcal{R}_{10} > 1$, Chagas disease can persist in the absence of *T.*

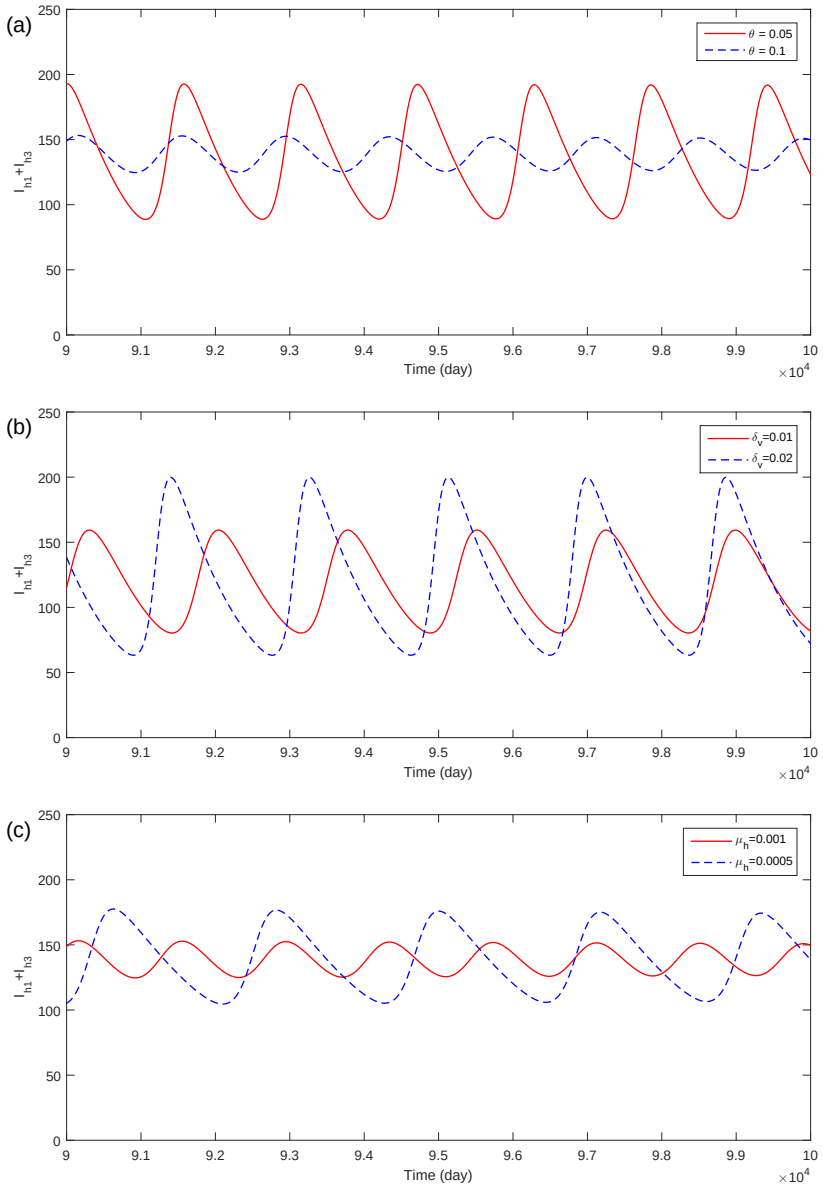

FIGURE 6. **(Color online) The effect of θ, δ_v and μ_h on the oscillation pattern of Chagas disease.** All simulations run until the steady state. Apart from the varied parameters in each subfigure, other associated parameters are fixed as $a = 0.6$, $b^{h1}_{1\to 0} = 0.06$, $b^{v1}_{1\to 0} = 0.2$, $b^{h2}_{2\to 0} = 0.05$, $b^{v2}_{2\to 0} = 0.2$, $N_h = 400$, $\mu_v = 0.005$, $r = 0.0274$, $\sigma = 0.001$, $\delta_v = 0.0347$, $\theta = 0.1$, $\mu_h = 0.001$.

rangeli infection, while with its presence, it is numerically found that Chagas disease can change from persistence to extinction if the invasion reproduction number $\mathcal{R}_{12} < 1$ (Fig. 4). Consequently, *T. rangeli* is a good sister trypanosome facilitating the risk reduction of Chagas disease dissemination.

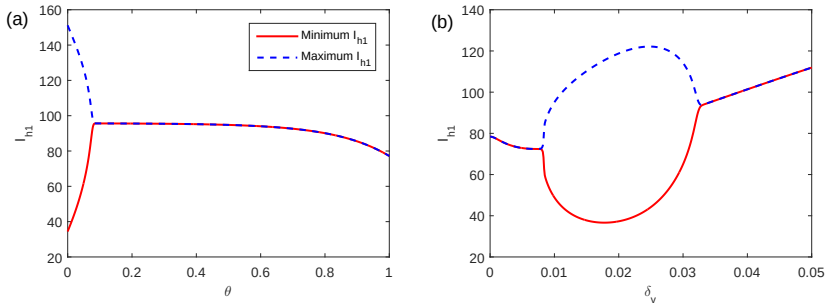

FIGURE 7. **(Color online) Numerical illustration of bifurcation diagram with the variation of θ and δ_v.** (a) Maximum/minimum sizes of I_{h1} at steady state with respect to $\theta \in [0, 1]$; (b) maximum/minimum sizes of I_{h1} at steady state with respect to $\delta_v \in [0, 0.05]$. Here, $a = 0.6$, $b^{h1}_{1\to 0} = 0.06$, $b^{v1}_{1\to 0} = 0.2$, $b^{h2}_{2\to 0} = 0.05$, $b^{v2}_{2\to 0} = 0.2$, $N_h = 400$, $\mu_h = 0.001$, $\mu_v = 0.005$, $r = 0.0274$, $\sigma = 0.001$ and $\delta_v = 0.0347$ for (a), $\theta = 0.1$ for (b) are used.

Though we have found that both parasites can uniformly persistent in the case of $\mathcal{R}_{20} > 1$, $\mathcal{R}_{10} > 1$ and $\mathcal{R}_{12} > 1$, while the dynamical behavior of Chagas disease can be completely different. With some reliable biological parameter values from Table 1, we have obtained that *T. cruzi*-infected host and triatomine bug populations either tend to the stable state (Fig. 5) or undergo oscillation phenomenon (Fig. 6), implying the co-infection model of Chagas disease has a rich dynamical behavior. Moreover, with the help of *T. rangeli* involved co-infection, the risk of Chagas disease infection is reduced since the corresponding sizes at endemic level are decreased (Fig. 5). Additionally, it is basically common for the occurrence of oscillation for vector-borne disease transmission since a number of factors such as maturation time delay, seasonality and annual spraying with insecticides could be major underlying mechanisms [31, 42, 47]. In this work, we have found another mechanism that *T. rangeli*-infected pathogenic effect on triatomine bugs can induce the occurrence of fluctuation as shown in Fig. 6, where both parameters θ and δ_v play an important role. Due to the complexity of model (2), we cannot find the robust analytical threshold condition for the occurrence of oscillation, but we have provided the numerical observation of bifurcation diagrams to identify the threshold condition as shown in Fig. 7. It is interesting and unexpected that neither low or high value of *T. rangeli*-infected death rate δ_v would stimulate the oscillation of Chagas disease, which will be left for future investigation.

However, a limitation is that we have ignored the Chagas disease induced death rate of host population in the formulated model which may not be necessarily correct. Though the dynamics may have some discrepancy, the numerical simulation results of basic and invasion reproduction numbers, size of each population at endemic equilibrium and/or oscillation state should be close. The solutions from the developed model should remain a good approximation to Chagas disease transmission. Another limitation is that for the assumption (6), where we assume that a dually-infected individual has a mild or weak interaction of the two parasites, and whether a dually-infected individual can transmit each parasite more or less efficiently than an individual infected with a single parasite have not been taken into

account. Moreover, how the different pathogenicity on single *T. rangeli*-infected and dually-infected triatomine bugs influence the Chagas disease spread is not fully studied here. In addition, host predation on bugs is another significant transmission means of *T. cruzi*. Moreover, vectors infected *T. rangeli* can lead to increased probing and hosts infected with *T. rangeli* can lead to increased predation [12, 24, 25, 32]. All these factors will jointly influence the dynamics of Chagas disease transmission. Nevertheless, due to mathematical challenge, the current model for the co-infection with *T. cruzi* and *T. rangeli* does not include the transmission route of host predation on vectors. We will address the effects of these important factors in a future work. In conclusion, this study provides some new insights beneficial to the prevention and control of Chagas disease. In general, with the involvement of sister trypanosoma *T. rangeli* co-infection, the risk of Chagas disease transmission is largely reduced.

Acknowledgments. We would like to thank the editors and two anonymous referees for their careful reading and helpful comments which have greatly improved the presentation of this paper.

REFERENCES

[1] M. A. Acuña-Zegarra, D. Olmos-Liceaga and J. X. Velasco-Hernández, The role of animal grazing in the spread of Chagas disease, *J. Theor. Biol.*, **457** (2018), 19–28.

[2] N. Añez, M. Molero, E. Valderrama, D. Nieves, et al., Studies on Trypanosoma rangeli Tejera, 1920 X- Its comparison with Trypanosoma cruzi Chagas, 1909. Infection in different stages of Rhodnius prolixus Stal, 1859, *KASMERA*, **20** (1992), 35–51.

[3] B. Basso, I. Castro, V. Introini, P. Gilb, C.Truyensc and E. Morettia, Vaccination with *Trypanosoma rangeli* reduces the infectiousness of dogs experimentally infected with *Trypanosoma cruzi*, *Vaccine*, **25** (2007), 3855–3858.

[4] B. Basso, E. Moretti and R. Fretes, Vaccination with epimastigotes of different strains of *Trypanosoma rangeli* protects mice against *Trypanosoma cruzi* infection, *Mem. Inst. Oswaldo Cruz.*, **103** (2008), 370–374.

[5] B. Basso, E. Moretti and R. Fretes, Vaccination with *Trypanosoma rangeli* induces resistance of guinea pigs to virulent *Trypanosoma cruzi*, *Vet. Immunol. Immunopathol.*, **157** (2014), 119–123.

[6] B. Basso, E. Moretti and E. Votrero-cima, Immune response and *Trypanosoma cruzi* infection in *Trypanosoma rangeli*-immunized mice, *Am. J. Trop. Med. Hyg.*, **44** (1991), 413–419.

[7] C. Barbu, E. Dumonteil and S. Gourbiére, Optimization of control strategies for nondomiciliated *Triatoma dimidiata*, Chagas disease vector in the Yucatan Peninsula, Mexico, *PLoS. Negl. Trop. Dis.*, **3** (2009), e416.

[8] G. Cruz-Pacheco, L. Esteva and C. Vargas, Control measures for Chagas disease, *Math. Biosci.*, **237** (2012), 49–60.

[9] A. B. B. de Oliveira, K. C. C. Alevi, C. H. L. Imperador, et al., Parasite-vector interaction of Chagas disease: A mini-review, *Am. J. Trop. Med. Hyg.*, **98** (2018), 653–655.

[10] O. Diekmann, J. A. P. Heesterbeek and J. A. J. Metz, On the definition and the computation of the basic reproduction ratio R_0 in models for infectious diseases in heterogeneous populations, *J. Math. Biol.*, **28** (1990), 365–382.

[11] O. Diekmann, J. A. P. Heesterbeek and M. G. Roberts, The construction of next-generation matrices for compartmental epidemic models, *J. R. Soc. Interface*, **7** (2010), 873–885.

[12] D. Erazo, et al., Modelling the influence of host community composition in a sylvatic Trypanosoma cruzi system, *Parasitology*, **144** (2017), 1881–1889.

[13] C. A. Eva, P. S. Katia, R. B. Giselle, et al., Nanocarriers for effective delivery of benznidazole and nifurtimox in the treatment of chagas disease: A review, *Acta. Tropica*, **198** (2019), 105080.

[14] M. R. Fellet, M. G. Lorenzo, S. L. Elliot, et al., Effects of infection by *Trypanosoma cruzi* and *Trypanosoma rangeli* on the reproductive performance of the vector *Rhodnius prolixus*, *PLoS One*, **9** (2014), e105255.

[15] R. C. Ferreira, C. F. Teixeira, V. F. A. de Sousa and A. A. Guarneri, Effect of temperature and vector nutrition on the development and multiplication of *Trypanosoma rangeli* in *Rhodnius prolixus*, *Parasitol. Res.*, **117** (2018), 1737–1744.
[16] D. Gao, T. C. Porco and S. Ruan, Coinfection dynamics of two diseases in a single host population, *J. Math. Anal. Appl.*, **442** (2016), 171–188.
[17] N. Gottdenker, L. Chaves, J. Calzada, et al., *Trypanosoma cruzi* and *Trypanosoma rangeli* co-infection patterns in insect vectors vary across habitat types in a fragmented forest landscape, *Parasitology*, **2** (2016), E10.
[18] M. J. Grijalva, V. Suarez-Davalos, A. G. Villacis et al., Ecological factors related to the widespread distribution of sylvatic Rhodnius ecuadoriensis populations in southern Ecuador, *Parasit. Vectors*, **5** (2012), 17.
[19] A. A. Guarneri and M. G. Lorenzo, Triatomine physiology in the context of trypanosome infection, *J. Insect Physiol.*, **97** (2017), 66–76.
[20] F. Guhl, L. Hudson, C. J. Marinkelle, et al., Clinical *Trypanosoma rangeli* infection as a complication of Chagas' disease, *Parasitology*, **94** (1987), 475–484.
[21] R. E. Gürtler, L. A. Ceballos, P. Ordóñez-Krasnowski et al., Strong host-feeding preferences of the vector Triatoma infestans modified by vector density: Implications for the epidemiology of Chagas disease, *PLoS Negl. Trop. Dis.*, **3** (2009), e447.
[22] R. E. Gürtler, U. Kitron, M. C. Cecere, et al., Sustainable vector control and management of Chagas disease in the Gran Chaco, Argentina, *Proc. Natl. Acad. Sci. USA.*, **104** (2007), 16194–16199.
[23] C. M. Kribs and C. Mitchell, Host switching vs. host sharing in overlapping sylvatic *Trypanosoma cruzi* transmission cycles, *J. Biol. Dyn.*, **9** (2015), 247–277.
[24] C. Kribs-Zeleta, Vector Consumption and Contact Process Saturation in Sylvatic Transmission of *T. cruzi*, *Mathematical Population Studies*, **13** (2006),135–152.
[25] C. Kribs-Zeleta, Estimating Contact Process Saturation in Sylvatic Transmission of *Trypanosoma cruzi* in the United States, *PLoS. Negl. Trop. Dis.*, **4** (2010), e656.
[26] M. Z. Levy, F. S. Malaga Chavez, J. G. Cornejo Del Carpio, et al., Rational spatio-temporal strategies for controlling a Chagas disease vector in urban environments, *J. R. Soc. Interface.*, **7** (2010), 1061–1070.
[27] B. Y. Lee, K. M. Bacon, A. R. Wateska, et al., Modeling the economic value of a Chagas disease therapeutic vaccine, *Hum. Vaccin. Immunother.*, **8** (2012), 1293–1301.
[28] B. Y. Lee, K. M. Bacon, M. E. Bottazzi and P. J. Hotez, Global economic burden of Chagas disease: A computational simulation model, *Lancet. Infect. Dis.*, **13** (2013), 342–348.
[29] B. Y. Lee, S. M. Bartsch, L. Skrip, et al., Are the London Declaration's 2020 goals sufficient to control Chagas disease?: Modeling scenarios for the Yucatan Peninsula, *PLoS Negl. Trop. Dis.*, **12** (2018), e0006337.
[30] K. C. F. Lidani, F. A. Andrade, L. Bavia, et al., Chagas disease: From discovery to a worldwide health problem, *Front. Public Health*, **7** (2019), 166.
[31] Y. Lou, J. Wu and X. Wu, Impact of biodiversity and seasonality on Lyme-pathogen transmission, *Theor. Biol. Med. Model.*, **11** (2014), 50.
[32] N. P. Marliére, M. G. Lorenzo and A. A. Guarneri, Trypanosoma rangeli infection increases the exposure and predation endured by Rhodnius prolixus, *Parasitology*, **149** (2022) 155–160.
[33] M. Martcheva and S. S. Pilyugin, The role of coinfection in multidisease dynamics, *SIAM J. Appl. Math.*, **66** (2006), 843–872.
[34] J. K. Peterson, S. M. Bartsch, B. Y. Lee and A. P. Dobson, Broad patterns in domestic vector-borne *Trypanosoma cruzi* transmission dynamics: Synanthropic animals and vector control, *Parasites Vectors*, **8** (2015), 537.
[35] J. K. Peterson, A. L. Graham, R. J. Elliott, A. P. Dobson and O. T. Chávez, *Trypanosoma cruzi-Trypanosoma rangeli* co-infection ameliorates negative effects of single trypanosome infections in experimentally infected *Rhodnius prolixus*, *Parasitology*, **143** (2016), 1157–1167.
[36] J. E. Rabinovich, J. A. Leal and D. Feliciangeli de Piñero, Domiciliary biting frequency and blood ingestion of the Chagas's disease vector *Rhodnius prolixus Stahl* (Hemiptera: Reduviidae), in Venezuela, *Trans. R. Soc. Trop. Med. Hyg.*, **73** (1979), 272–283.
[37] A. Requena-Méndez, E. Aldasoro, E. de Lazzari, et al., Prevalence of Chagas disease in Latin-American migrants living in Europe: A systematic review and meta-analysis, *PLoS Negl. Trop. Dis.*, **9** (2015), e0003540.
[38] W. E. Ricker, *Computation and Interpretation of Biological Statistics of Fish Populations*, *Bull. Fish. Res. Board Can.*, No. 191, Blackburn Press, Ottawa, 1975.

[39] J. M. Sánchez, S. O. Beffi Sueto, P. Schwabl, M. J. Grijalva, M. S. Llewellyn and J. A. Costales, Remarkable genetic diversity of *Trypanosoma cruzi* and *Trypanosoma rangeli* in two localities of southern Ecuador identified via deep sequencing of mini-exon gene amplicons, *Parasites Vectors*, **13** (2020), 252.
[40] H. L. Smith, *Monotone Dynamical Systems: An Introduction to the Theory of Competitive and Cooperative Systems*, *Am. Math. Soc. Math. Surv. Monogr.*, 1995.
[41] H. L. Smith and P. Waltman, *The Theory of the Chemostat*, Cambridge University Press, 1995.
[42] A. M. Spagnuolo, M. Shillor, L. Kingsland, et al., A logistic delay differential equation model for Chagas disease with interrupted spraying schedules, *J. Biol. Dyn.*, **6** (2012), 377–394.
[43] H. R. Thieme, Persistence under relaxed point-dissipativity (with application to an endemic model), *SIAM J. Math. Anal.*, **24** (1993), 407–435.
[44] N. Tomasini, P. G. Ragone, S. Gourbiére, et al., Epidemiological modeling of *Trypanosoma cruzi*: Low stercorarian transmission and failure of host adaptive immunity explain the frequency of mixed infections in humans, *PLoS Comput. Biol.*, **13** (2017), e1005532.
[45] P. van den Driessche and J. Watmough, Reproduction numbers and sub-threshold endemic equilibria for compartmental models of disease transmission, *Math. Biosci.*, **180** (2002), 29–48.
[46] J. X. Velasco-Hernández, An epidemiological model for the dynamics of Chagas disease, *Biosystems*, **26** (1991), 127–134.
[47] J. X. Velasco-Hernández, A model for Chagas disease involving transmission by vectors and blood transfusion, *Theor. Popul. Biol.*, **46** (1994), 1–31.
[48] A. G. Villacís, S. Ocaña-Mayorga, M. S. Lascano, C. A. Yumiseva, E. G. Baus and M. J. Grijalva, Abundance, natural infection with trypanosomes, and food source of an endemic species of triatomine, Panstrongylus howardi (Neiva 1911), on the Ecuadorian Central Coast, *Am. J. Trop. Med. Hyg.*, **92** (2015), 187–192.
[49] World Health Organization, Chagas disease (American trypanosomiasis), *Available at:* https://www.who.int, Accessed 12 June 2020.
[50] X. Wu, D. Gao, Z. Song and J. Wu, Modelling triatomine bug population and *Trypanosoma rangeli* transmission dynamics: Co-feeding, pathogenic effect and linkage with Chagas disease, *Math. Biosci.*, **324** (2020), 108326.
[51] X.-Q. Zhao, Uniform persistence and periodic coexistence states in infinite-dimensional periodic semiflows with applications, *Can. Appl. Math. Q.*, **3** (1995), 473–495.

Received July 2021; revised April 2022; early access June 2022.

E-mail address: xtwu@shmtu.edu.cn
E-mail address: dzgao@shnu.edu.cn
E-mail address: buctsongzilong@163.com
E-mail address: wujh@yorku.ca